Available online at www.sciencedirect.com
SCIENCE DIRECT®
Surface Science 583 (2005) 179–190
SURFACE SCIENCE
www.elsevier.com/locate/susc

Room-temperature chemisorption and thermal evolution of perchloroethylene and trichloroethylene on Si(1 1 1)7 × 7: Formation of chlorinated vinylene and vinylidene and acetylide adspecies, and thermal etching reactions

Zhenhua He, K.T. Leung *

Department of Chemistry, University of Waterloo, 200 University Ave. West, Waterloo, ON, Canada N2L 3G1

Received 9 December 2004; accepted for publication 18 March 2005
Available online 13 April 2005

Abstract

The prominent surface species and their corresponding bonding structures of perchloroethylene (PCE, C_2Cl_4) and trichloroethylene (TCE, C_2HCl_3) upon room-temperature adsorption and thermal excitation on Si(1 1 1)7 × 7 have been examined by vibrational electron energy loss spectroscopy (EELS) and thermal desorption spectrometry (TDS). The presence of the Si–Cl stretch at 510 cm^{-1} shows that both PCE and TCE undergo dechlorination on Si(1 1 1)7 × 7, while the presence of the C=C stretch near 1500 cm^{-1} indicates that the C=C bond remains intact upon adsorption. The mono-σ bonded trichlorovinyl ($Cl\dot{C}{=}CCl_2$) and 1,2-dichlorovinyl ($Cl\dot{C}{=}CHCl$) adspecies have been proposed as plausible adsorption intermediates for PCE and TCE, respectively. Furthermore, the trichlorovinyl adspecies is found to further dechlorinate at 350 K, and becomes carbon clusters and/or SiC after complete dechlorination above 450 K. On the other hand, further dechlorination of the dichlorovinyl adspecies above 350 K is found to produce a di-σ bonded chlorovinylene adspecies that is stable up to 450 K. As supported by the presence of the C≡C stretch at 3300 cm^{-1}, an additional adspecies in the form of acetylide ($\dot{C}{\equiv}CH$) is also observed. Above 580 K, hydrocarbon fragments and/or SiC are evident, likely due to dehydrogenation of the chlorovinylene and acetylide adspecies. In addition to these novel adspecies, our TDS data reveal desorption of $SiCl_2$ over 800–950 K and HCl over 700–900 K for both PCE and TCE, which supports thermal etching and recombinative dehydrochlorination reactions at a higher temperature. The TDS data also provide evidence for weak molecular adsorption, likely related to dative bonding as a result of inductive effects.

Keywords: Chemisorption; Dechlorination; Chloroethylenes; Si(1 1 1)7 × 7; Electron energy loss spectroscopy; Thermal desorption spectrometry

* Corresponding author. Tel.: +1 5198884567x5826; fax: +1 5197460435.
E-mail address: tong@uwaterloo.ca (K.T. Leung).

0039-6028/$ - see front matter
doi:10.1016/j.susc.2005.03.037

1. Introduction

Halogenated hydrocarbons are widely used in semiconductor industry. For example, tetrachloroethylene or perchloroethylene (PCE, $Cl_2C{=}CCl_2$) and trichloroethylene (TCE, $Cl_2C{=}CHCl$) have been used as precursor gases in SiC alloys formation by electron cyclotron resonance chemical vapour deposition to reduce the hydrogen content and to improve the microstructure of the silicon carbide films [1]. *Trans*-dichloroethylene and TCE have also been used as a Cl source to reduce metal contamination during Si oxidation [2,3]. Chlorinated hydrocarbons also attract a lot of attention not only as common industrial solvents but also as potential precursors in photochemical etching of semiconductor surfaces [4–7]. Although the binding and surface chemistry of halobenzenes on Si single-crystal surfaces have been investigated [6–9], not much is known about the basic interactions of halogenated derivatives of the simplest unsaturated hydrocarbon (halogenated ethylenes) with the Si surface. Recently, our group has started a series of systematic studies of surface chemical processes of the halogenated ethylenes on Si(1 1 1) and Si(1 0 0) surfaces by using vibrational electron energy loss spectroscopy (EELS) [10], X-ray photoelectron spectroscopy (XPS) [11], and thermal desorption spectrometry (TDS). These studies led us to hypothesize the plausible existence of novel adspecies involving unique bonding structures, including vinylene and vinylidene [10]. As our continuing effort to examine the basic interactions of halogenated hydrocarbons with Si single-crystal surfaces and related novel surface species, we now present a more detailed study of the room-temperature (RT) adsorption properties of PCE and TCE and the thermal evolution of the resulting adspecies on Si(1 1 1)7×7 by using vibrational EELS and TDS. Given that PCE does not contain any H atom while TCE contains only one H atom, the difference in the H content provides easy identification of the adspecies by comparing their corresponding EELS spectra. Furthermore, PCE (with a D_{2h} symmetry) has a higher molecular symmetry than TCE (C_s), which makes these molecules a good testing ground for studying the effects of molecular symmetry (and related structural dipole) on the surface chemistry of silicon. Because both PCE and TCE are popular industrial solvents and common contaminants in drinking water, better understanding of the adsorption and surface chemistry of PCE and TCE and the development of new dechlorination methods [12] would also be of practical interest to environmental studies and groundwater research.

2. Experimental setup

The experimental apparatus and procedure used in the present work have been described in detail elsewhere [13]. Briefly, the experiments were conducted in a home-built ultrahigh vacuum (UHV) system with a base pressure better than 5×10^{-11} Torr. All of the EELS measurements were made with the sample held at RT under specular reflection scattering condition of 45° from the surface normal. A routine energy resolution of 12–17 meV (or 97–136 cm^{-1}) full-width at half-maximum with a typical count rate of 100,000 counts per second for the elastic peak could be achieved with our spectrometer operated at 5 eV impact energy. It should be noted that the calibration and tuning of the EELS spectrometer typically limited the reproducibility of the measured peak positions to ±2 meV (or ±16 cm^{-1}) in the present work. The TDS experiments were obtained by using a differentially pumped quadrupole mass spectrometer (QMS) to monitor the ion fragments, along with a home-built programmable proportional–integral–differential temperature controller to provide a linear heating rate of 1 K s^{-1}. The Si(1 1 1) sample (p-type boron-doped, 50 Ω cm, 8×6 mm^2, 0.5 mm thick) with a stated purity of 99.999% was purchased from Virginia Semiconductor Inc. The sample was mechanically fastened to a Ta sample plate with Ta wires (0.25 mm diameter) and could be annealed by electron bombardment from a heated tungsten filament at the backside of the sample. The Si sample was cleaned by a standard procedure involving repeated cycles of Ar^+ sputtering and annealing to 1200 K until a sharp 7×7 LEED pattern was observed. The cleanliness of the 7×7 surface was further verified

in situ by the lack of any detectable vibrational EELS feature attributable to unwanted contaminants, particularly the Si–C stretching mode at 800–850 cm^{-1}. Perchloroethylene (99.9% purity) and trichloroethylene (99.5% purity) were purchased from Sigma-Aldrich and used without further purification after appropriate degassing by repeated freeze–pump–thaw cycles. The clean Si(1 1 1) sample was exposed to the appropriate chloroethylene vapours at a typical (uncalibrated) pressure of 1×10^{-6} Torr by using a variable leak valve. All exposures were reported in units of Langmuir (1 L = 1×10^{-6} Torr s).

3. Results and discussion

3.1. Room-temperature chemisorption of PCE and TCE on Si(1 1 1)7 × 7

Fig. 1 shows the vibrational EELS spectra of PCE on Si(1 1 1)7 × 7 as a function of exposure at RT. Evidently, the clean Si(1 1 1)7 × 7 surface is characterized by a loss continuum in the corresponding EELS spectrum (Fig. 1a). The loss continuum is mainly attributed to the excitations of two-dimensional plasmons associated with the dangling-bond electrons and to low-lying interband and intraband transitions with significant electron–phonon coupling [14–16]. Upon exposure of the adsorbates, the loss continuum becomes reduced, indicating the involvement of the dangling-bond electrons in the chemisorption process. For PCE, three EELS features at 1490 cm^{-1}, 820 cm^{-1}, and 510 cm^{-1} are evident and the intensities of these features become saturated above 40 L (Fig. 1). To facilitate spectral assignments, we compare the surface vibrational EELS data obtained in the present work with the corresponding infrared and Raman spectroscopic data of chloroethylenes obtained in the gas or liquid phase [17–20]. The features observed at 1490 cm^{-1}, 820 cm^{-1} and 510 cm^{-1} can be assigned predominantly to the C=C, C–Cl, and Si–Cl stretching modes, respectively. In accord with the characteristic frequency for the Si–Cl stretching mode commonly found in 467–600 cm^{-1} [21,22], the prominent feature observed at 510 cm^{-1} can therefore be used to indicate the relative surface Cl moiety and the degree of dechlorination upon adsorption. The presence of other vibrational modes such as various lower-lying CCl_2 bending modes may obscure the feature observed at 510 cm^{-1} [21]. The dissociation of Cl from PCE is also supported by the evolution of the sharp 7 × 7 LEED pattern for the clean Si(1 1 1) surface to a diffuse 7 × 7 and eventually 1 × 1 pattern upon a saturation exposure. The plausible adspecies as a result of single dechlorination of PCE could only be the mono-σ bonded trichlorovinyl ($ClC{=}CCl_2$) adspecies, which could further dechlorinate to a di-σ bonded dichlorovinylidene ($>C{=}CCl_2$) or dichlorovinylene (ClC=CCl) adspecies.

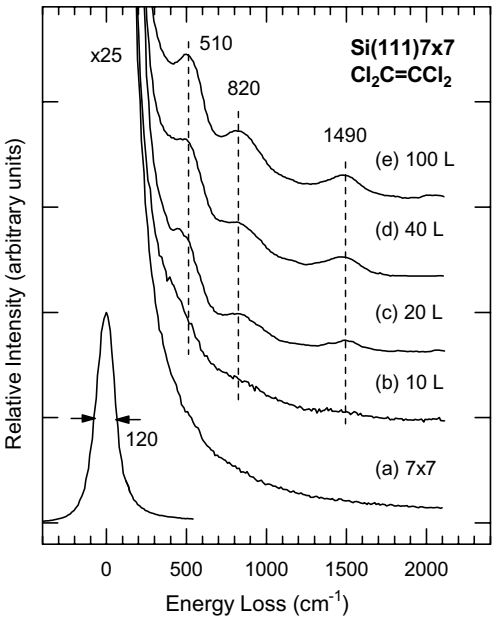

Fig. 1. Vibrational electron energy loss spectra for perchloroethylene exposed to (a) Si(1 1 1)7 × 7 at room temperature as a function of exposure: (b) 10 L, (c) 20 L, (d) 40 L, and (e) 100 L.

Fig. 2 shows the vibrational EELS spectra of TCE on Si(1 1 1)7 × 7 as a function of exposure at RT, which exhibit exposure dependence and change from a 7 × 7 to 1 × 1 LEED pattern similar to those found for PCE upon saturation exposure to above 40 L. In addition to the features at 1510 cm^{-1}, 820 cm^{-1} and 510 cm^{-1} which can be assigned respectively to C=C, C–Cl and Si–Cl

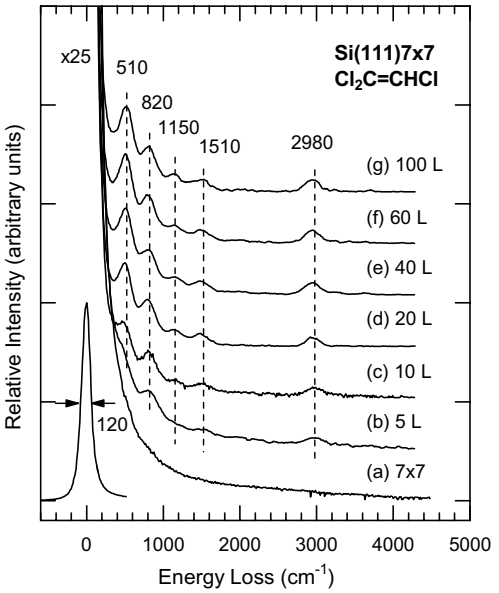

Fig. 2. Vibrational electron energy loss spectra for trichloroethylene exposed to (a) Si(1 1 1)7 × 7 at room temperature as a function of exposure: (b) 5 L, (c) 10 L, (d) 20 L, (e) 40 L, (f) 60 L, and (g) 100 L.

stretching modes (as for the PCE case in Fig. 1), the two additional features at 2980 cm^{-1} and 1150 cm^{-1} for the TCE sample can be attributed to the C–H stretching and CH in-plane bending modes, respectively. These assignments are in general accord with those for the gas-phase data [17–19]. The presence of the C=C stretch at 1510 cm^{-1} is clearly established for TCE (and PCE) without the presence of neighbouring CH_2 scissoring modes that often obscure this region in the case of other hydrocarbons [17,21]. Like the PCE case (Fig. 1), the presence of the Si–Cl stretching mode at 510 cm^{-1} indicates Cl dissociation for TCE. On the other hand, the absence of the Si–H stretching mode near 2100 cm^{-1} shows that C–H bond cleavage is not the preferred route upon RT adsorption of TCE on Si(1 1 1)7 × 7. The plausible surface species could then include the mono-σ bonded 2,2-dichlorovinyl ($H\dot{C}{=}CCl_2$) and 1,2-dichlorovinyl ($Cl\dot{C}{=}CHCl$) adspecies (with two conformers). The two conformers of the 1,2-dichlorovinyl adspecies depend on whether the Cl atom on the non-ipso (or beta) C atom is closer to the surface (*trans* form) or not (*cis* form), which are similar to the respective analogous adstructures for *trans*- and *cis*-dichloroethylene ($H\dot{C}{=}CHCl$) [10]. These 2,2-dichlorovinyl and 1,2-dichlorovinyl adspecies could undergo further dechlorination (but evidently not dehydrogenation) to chlorovinylene ($H\dot{C}{=}\dot{C}Cl$) and chlorovinylidene (>C=CHCl), respectively. It should be noted that the preferred Cl dissociation over H abstraction is generally consistent with the stronger bond strength of Si–Cl (377 kJ mol^{-1}) relative to C–Cl (339 kJ mol^{-1}) [23–25]. The generally stronger C–H bond strength (414 kJ mol^{-1}) relative to Si–H bond strength (314 kJ mol^{-1}) [23–25] also supports the lack of H abstraction in the present case. For the adsorption of multiply chlorinated hydrocarbons on Cu(1 0 0), Yang et al. found that C–Cl bond cleavage is more facile in the $>CCl_2$ groups than the >CHCl group and that the scission of the first C–Cl bond is followed by rapid alpha or beta chlorine elimination near RT [26]. The observed preference for the initial adsorption via Cl dissociation through the $>CCl_2$ group by Yang et al. [26] suggests that the 1,2-dichlorovinyl ($Cl\dot{C}{=}CHCl$) adspecies would therefore be the preferred initial adsorption structure on Si(1 1 1)7 × 7. This preference could also be understood in terms of the polarity of the adsorbate and the relative electronegativity of the substrate Si atoms. However, the follow-up chlorine elimination as observed on Cu(1 0 0) [26] would not be feasible on Si(1 1 1)7 × 7 at RT because the Si–Si bond distances between Si atoms with dangling bonds are not physically compatible for further Cl abstraction from the non-ipso C. In particular, the distances between two adatoms (6.65–7.68 Å) and between an adatom and a rest-atom (4.56 Å) on the 7 × 7 surface [27,28] are considerably greater than the molecular dimension of TCE with C=C and C–Cl bond lengths of 1.34 Å and 1.73 Å respectively [29]. Although breakage of the back-bond (between an adatom and a pedestal atom with a typical separation of 2.36 Å [28,29]) has been proposed earlier as a viable mechanism for the adsorption of electronegative adsorbates [30,31], such a process would be more likely at elevated temperatures. In our earlier work, we also observed that the saturation exposures for *cis*- and *trans*-dichloroethylene on the 7 × 7 surface

(>600 L) to be considerably higher than that for *iso*-dichloroethylene (~10 L) [10], which suggests that the structure of the latter 1,2-dichlorovinyl (ClĊ=CHCl) adspecies is likely the more prominent structure, confirming the preference for adsorption via Cl dissociation on the CCl_2 side.

The intensity ratio of the Si–Cl stretch feature at 510 cm^{-1} relative to the C=C stretch feature at 1510 cm^{-1} for a 100 L exposure of TCE (3.9, Fig. 2g) is discernibly larger than the corresponding intensity ratio of the feature at 510 cm^{-1} to that at 1490 cm^{-1} for a 100 L exposure of PCE (2.0, Fig. 1e). The intensities of individual features have been estimated by using a least-square curve-fitting routine with Gaussian lineshapes. This difference in the relative intensity ratios indicates either enhanced dechlorination for TCE or the presence of a plausible molecular adsorption channel for PCE (see below). However, the relative amounts of dechlorination for both TCE and PCE are expected to be similar due to the preference for single dechlorination at the CCl_2 side upon the initial adsorption, which is supported by the similar peak intensities found for the Si–Cl stretch features relative to the respective elastic peaks for both TCE (Fig. 2g) and PCE (Fig. 1e). On the other hand, differences in the amounts of molecularly adsorbed species could account at least in part for the observed differences in the relative intensities. Without knowledge of the molecular adsorption structures and the respective dipole moments for the constituent bonding components in the molecular and dechlorinated adstructures, it is difficult to further ascertain the respective surface moieties of these adstructures.

It should be noted that post-oxidation of the exposed samples does not affect the respective EELS spectra (not shown), which indicates that the adsorption of PCE and TCE on Si(1 1 1)7 × 7 appears to have passivated the 7 × 7 surface, likely due to the Cl abstraction. Furthermore, exposure of PCE and TCE on an oxidized Si(1 1 1) surface at RT does not produce any EELS features attributable to PCE (Fig. 1) and TCE (Fig. 2), which suggests that the dangling bonds of the clean 7 × 7 surface are required for the initial adsorption of PCE and TCE. For an argon-sputtered Si(1 1 1) surface, the corresponding EELS features of PCE and TCE (not shown) generally become weaker and broader, suggesting a multitude of bonding sites with similar adsorption structures.

3.2. Thermal evolution of PCE and TCE on Si(1 1 1)7 × 7

Figs. 3 and 4 show respectively the TDS profiles of selected mass fragments for 100 L exposures of PCE and TCE to Si(1 1 1)7 × 7. It should be noted that the TDS data have been smoothed by adjacent averaging and the respective monotonically increasing backgrounds with increasing temperature have also been removed. For the PCE experiments, the presence of a weak desorption feature for mass 166 ($C_2{}^{35}Cl_3{}^{37}Cl^+$, corresponding to the base mass [32]) at 365 K (Fig. 3d), indicates molecular desorption. Of the other mass fragments monitored (masses 131, 129, 96, 94, 82, 59 and 47), the TDS profiles for mass 131 ($C_2{}^{35}Cl_2{}^{37}Cl^+$), mass 129 ($C_2{}^{35}Cl_3^+$), mass 96 ($C_2{}^{35}Cl^{37}Cl^+$), and mass 47 ($C^{35}Cl^+$) (not shown) also follow that of the

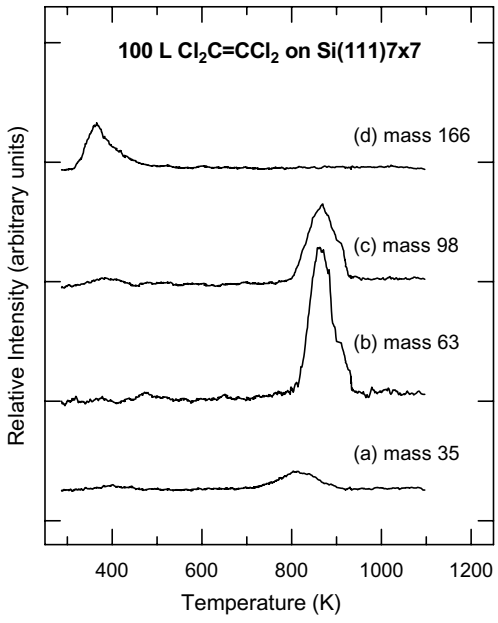

Fig. 3. Thermal desorption profiles of (a) mass 35 (Cl^+), (b) mass 63 ($SiCl^+$), (c) mass 98 ($SiCl_2^+$), and (d) mass 166 ($C_2Cl_4^+$) for 100 L of perchloroethylene exposed to Si(1 0 0)7 × 7 at room temperature.

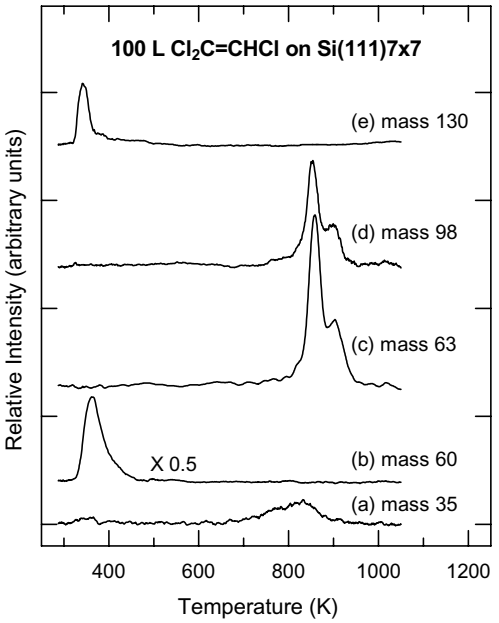

Fig. 4. Thermal desorption profiles of (a) mass 35 (Cl^+), (b) mass 60 (C_2HCl^+), (c) mass 63 ($SiCl^+$), (d) mass 98 ($SiCl_2^+$), and (e) mass 130 ($C_2HCl_3^+$) for 100 L of trichloroethylene exposed to Si(1 1 1)7 × 7 at room temperature.

base mass (Fig. 3d), indicating that these fragments originate from cracking of the desorbed parent mass in the ionizer of the QMS. Similarly, the TDS profile of the parent mass for TCE, mass 130 ($C_2H^{35}Cl_3^+$), also exhibits a desorption maximum at 340 K (Fig. 4e). The TDS profiles for the other monitored mass fragments of TCE (mass 97 ($C_2H^{35}Cl^{37}Cl^+$) and 95 ($C_2H^{35}Cl_2^+$)) (not shown) also follow that of the parent mass. Considerable efforts have been made to assure that the desorbed species come indeed from the Si sample instead of the sample holder, by positioning the front face of the sample as close as possible (within 1 mm) to the entrance of the differentially pumped housing of the QMS. Such an arrangement has been found to be effective in lowering the background and preventing the desorbed species in the surrounding from entering the ionizer region of the QMS. To eliminate the filament used for electron-beam sample heating of the backside of the sample as a possible source of the desorbed species, we irradiated the front face of the sample with low-energy electrons (50 eV kinetic energy) emitted from a heated tungsten filament located 5 cm away. The follow-up TDS experiments showed that the desorption features for the parent mass near 350 K are no longer present, which confirms that the desorbed molecular species are originated from the surface and not from the filament used for sample heating. The low desorption temperatures of the parent masses for both PCE and TCE (near 350 K) suggest that the molecularly desorbed species are from as-deposited (intact) molecules and not from recombinative desorption of dissociated adsorbed fragments, which would require a higher desorption temperature. In addition, the molecular desorption profile for PCE (Fig. 3d) is found to be considerably broader than that for TCE (Fig. 4e), suggesting the presence of a larger number of more dissimilar molecular adsorption states for PCE than TCE. This difference could be related to the difference in the molecular dipole resulting from different adsorption structures of the adsorbates. Evidently, the nonpolar PCE appears to have a less well-defined adsorption state on the Si(1 1 1)7 × 7 surface, in contrast to that for polar TCE.

We have also monitored the lower mass fragments, particularly mass 94 ($C_2{}^{35}Cl_2^+$) and mass 60 ($C_2H^{35}Cl^+$) for PCE and TCE respectively. In marked contrast to PCE for which no discernible desorption feature is found for mass 94 (not shown), an intense desorption feature of mass 60 at 360 K is clearly evident for TCE (Fig. 4b), which indicates the formation of chloroacetylene (C_2HCl) upon low-temperature annealing. This mass-60 desorption feature at 360 K (Fig. 4b) also appears to be considerably more intense than and it closely follows the molecular desorption peak at 340 K (Fig. 4e). It should be noted that the observed mass-60 desorption intensity relative to the parent mass (mass 130) is also greater than that found in the gas-phase cracking pattern of TCE [32]. A possible mechanism for the apparently enhanced production of chloroacetylene is the double dechlorination of the inductively bonded TCE, in which two Cl atoms are transferred from the molecularly bonded TCE to the substrate releasing the chloroacetylene. This mechanism is generally consistent with the propensity of TCE to dechlorinate on the Si surface (see below), likely

because of the stronger bond strength of Si–Cl (377 kJ mol^{-1}) than that of C–Cl (339 kJ mol^{-1}) [23–25]. The absence of any mass-94 desorption feature for PCE could be due to the lack of a dipole moment for PCE, in which case the inductive bonding of PCE to the Si surface is too weak to allow transfer of the Cl atoms to the surface and only molecular desorption is observed.

Figs. 3 and 4 also show the respective TDS features of mass 98 ($SiCl_2^+$) and mass 63 ($SiCl^+$) for both PCE and TCE. The main peak at 860 K and the shoulder at 900 K for these TDS profiles evidently correspond to two possible desorption states for these etching products. Earlier chemisorption studies of $SiCl_4$ and SiH_2Cl_2 on Si(1 0 0) and Si(1 1 1) surfaces have suggested that a lower-temperature state at 700 K could correspond to desorption of dichloride surface species while a higher-temperature state at 900 K may correspond to disproportionation of two monochloride species [33], although the nature of these states remain unclear in the present case. The similarity in the desorption temperatures for the two TDS features observed in the present work (i.e., 860 K and 900 K) therefore suggests that these features are more likely due to similar disproportionation processes of Cl atoms at two different sets of surface sites. The nearly identical profiles with similar desorption maxima for the mass 98 and mass 63 TDS features (with an intensity ratio of 1:1.8) also indicate that they originate from the same desorption product. Because $SiCl_2^+$ and $SiCl^+$ are found to be in comparable amounts from electron impact studies of gaseous $SiCl_2$ [34,35], the parent desorption species is likely $SiCl_2$. Furthermore, we have also monitored mass 133, corresponding to $SiCl_3^+$ of the heavier etching product $SiCl_4$, but found no desorption feature, confirming $SiCl_2$ as the main etching product. In addition, a weak and broad desorption peak of mass 35 (Cl^+) at 810 K is also observed in the TDS profiles for both PCE (Fig. 3a) and TCE (Fig. 4a), which indicates recombinative desorption of a small quantity of HCl upon thermal evolution. Although mass 36 (HCl^+) was also monitored, the weak feature was found to be easily obscured by the high background. In the case of PCE, the existence of a small amount of H atoms found on the Si surface is attributed to dissociation of residual water commonly present in UHV chambers [36].

In order to further investigate the decomposition products remaining on Si(1 1 1)7 × 7 upon thermal evolution of the adsorbed PCE and TCE molecules, we record EELS spectra for a 100 L RT exposure of PCE (shown in Fig. 5) and of TCE (shown in Fig. 6) on the 7 × 7 surface upon annealing the respective samples to different temperatures. We also provide in Fig. 7 a summary of our proposed thermal evolution pathways for PCE and TCE on the 7 × 7 surface, to better facilitate our discussion below. Evidently, both the C=C stretching mode at 1490 cm^{-1} and C–Cl stretching mode at 820 cm^{-1} for the PCE sample are found to be weaken upon annealing to 350 K (Fig. 5b) and they become essentially extinct at 450 K (Fig. 5c). On the other hand, the Si–Cl stretching mode at 510 cm^{-1} is found to be strengthen considerably upon annealing to 450 K (Fig. 5c). The reduction in the intensity of the C–Cl feature at 820 cm^{-1} and the corresponding increase in that of the Si–Cl feature at 510 cm^{-1}

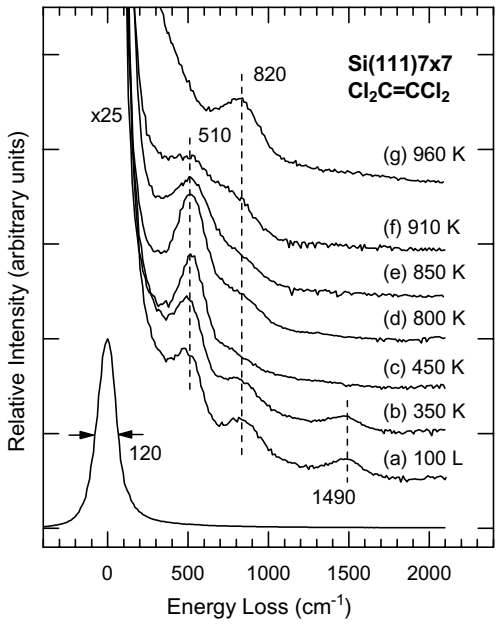

Fig. 5. Vibrational electron energy loss spectra for 100 L of perchloroethylene exposed to (a) Si(1 1 1)7 × 7 at room temperature, and upon annealing to (b) 350 K, (c) 450 K, (d) 800 K, (e) 850 K, (f) 910 K, and (g) 960 K.

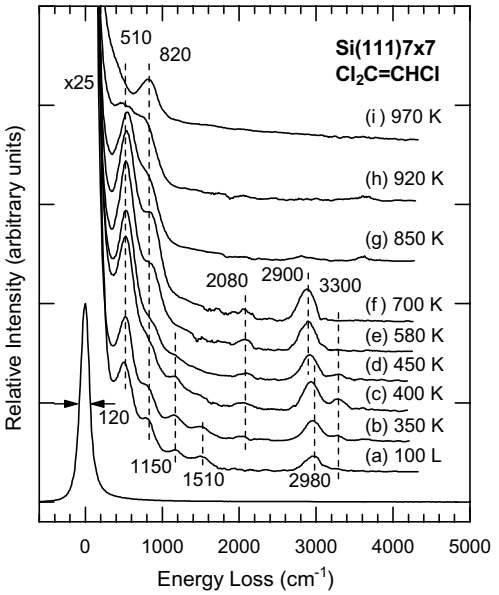

Fig. 6. Vibrational electron energy loss spectra for 100 L of trichloroethylene exposed to (a) Si(1 1 1)7 × 7 at room temperature, and upon annealing to (b) 350 K, (c) 400 K, (d) 450 K, (e) 580 K, (f) 700 K, (g) 850 K, (h) 920 K, and (i) 970 K.

confirm total dechlorination of the adspecies upon annealing to 450 K. Moreover, the extinction of the C=C stretching feature at 1490 cm^{-1} upon annealing to 450 K suggests the conversion of the mono-σ bonded trichlorovinyl ($ClC{=}CCl_2$) adspecies (Structure III, Fig. 7b) to the dichlorovinylene ($ClC{=}CCl$) adspecies (Structure IV, Fig. 7b), which becomes transparent to dipole excitation due to its near surface-parallel adsorption geometry (and the surface selection rule). Dechlorination of the trichlorovinyl adspecies to the surface-perpendicular dichlorovinylidene ($>C{=}CCl_2$) adspecies is not likely because such an adspecies would exhibit a strong C=C stretching mode, which is absent above 450 K. It is also of interest to note that the presence of the molecularly adsorbed PCE (Structure I, Fig. 7a) is also transparent to the EELS analysis due to its near surface-parallel adsorption configuration. Clearly, we cannot rule out the possibility of breakage of the C=C bond (with a bond energy of 611 kJ mol^{-1} [24,25]) and the formation of carbon clusters on the Si surface at the higher temperature.

Further annealing the PCE sample to 800 K is found to strengthen the Si–Cl stretching mode at 510 cm^{-1} slightly while a broad peak near 820 cm^{-1} attributable to Si–C stretching mode reappears (Fig. 5d). The Si–Cl stretching mode at 510 cm^{-1} continues to reduce in intensity upon continued annealing to 960 K (Fig. 5g), which indicates that the dissociated Cl atoms are being removed from the surface, in good accord with the desorption of the $SiCl_2$ species (mass 98) over 800–950 K (Fig. 3c) and HCl over 700–900 K (Fig. 3a) as observed in our TDS experiment. Concurrently, the intensity of the Si–C stretching mode at 820 cm^{-1} is found to increase dramatically upon annealing to 960 K (Fig. 5g), which indicates that only C atoms remain likely in the form of SiC (and/or carbon clusters) upon total dechlorination at these high temperatures (Fig. 7b).

Similar observations can be made for the thermal evolution of the Si–Cl stretch at 510 cm^{-1}, C–Cl stretch at 820 cm^{-1} and C=C stretch at 1510 cm^{-1} for a 100 L exposure of TCE on Si(1 1 1)7 × 7 at RT (Fig. 6). In particular, the reduction in the intensity of the C–Cl stretch at 820 cm^{-1} along with a concomitant increase in that of the Si–Cl stretch at 510 cm^{-1} (Fig. 6a–d) indicates that the proposed mono-σ bonded 1,2-dichlorovinyl ($ClC{=}CHCl$) adspecies, with two conformer structures represented by Structures VI and VII in Fig. 7d, continues to dechlorinate to chlorovinylene ($HC{=}CCl$, Structure VIII, Fig. 7d) and chlorovinylidene ($>C{=}CHCl$, Structure X, Fig. 7d) upon annealing to 450 K. However, the total elimination of the C=C stretch feature at 1510 cm^{-1} upon annealing to above 400 K (Fig. 6c) again suggests that the dipole-inactive surface-parallel bonded chlorovinylene (Structure VIII, Fig. 7d) is the preferred product over the dipole-active surface-perpendicularly bonded chlorovinylidene adspecies (Structure X, Fig. 7d). The intensity for the Si–Cl stretch feature at 510 cm^{-1} continues to grow upon annealing to 580 K (Fig. 6e), effectively in concert with the reduction in intensity of the C–Cl stretch at 820 cm^{-1}, which suggests breakage of the C–Cl bonds and the transfer of the Cl atoms onto the surface. Upon further annealing the sample to 970 K (Fig. 6i), the Si–Cl stretch feature at 510 cm^{-1} gradually diminishes,

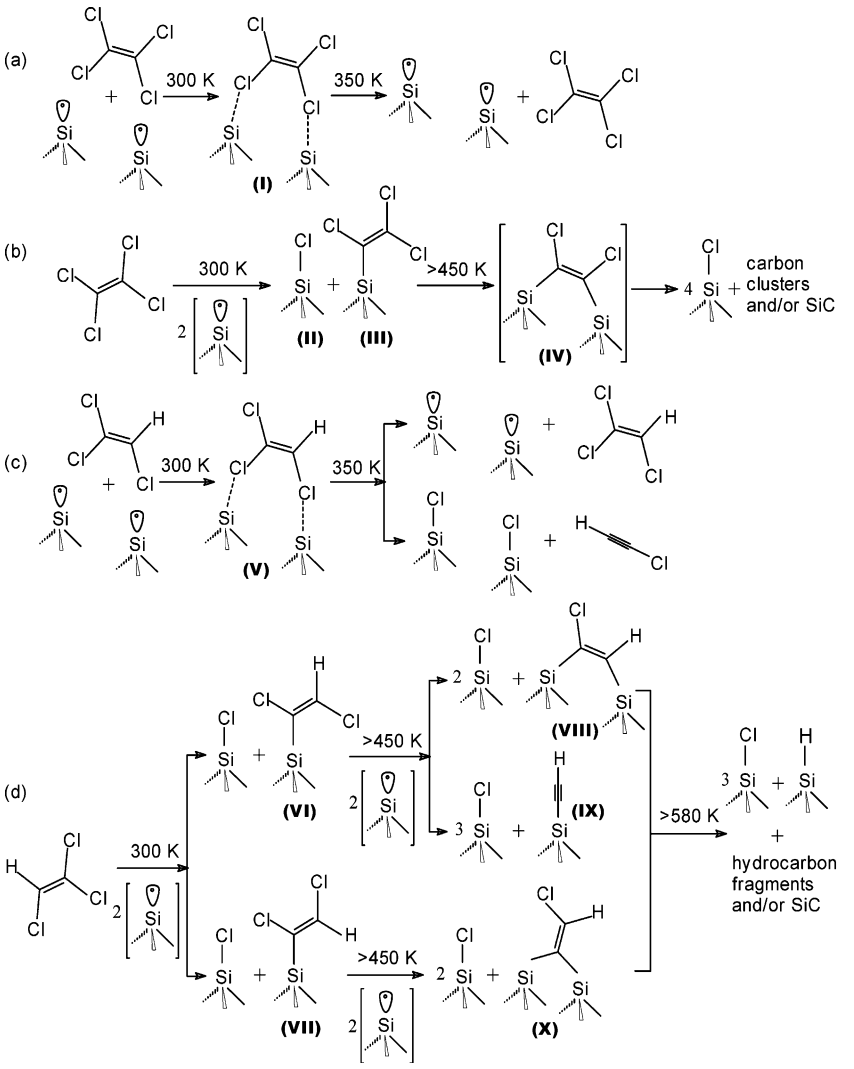

Fig. 7. Schematic diagrams of plausible adsorption structures and thermal evolution products for (a,b) perchloroethylene and (c,d) trichloroethylene exposed to Si(1 1 1)7 × 7 at room temperature.

which is in good accord with the desorption of the etching products $SiCl_2$ over 800–950 K (Fig. 4d) and HCl over 700–900 K (Fig. 4a) as shown in the corresponding TDS profiles. On the other hand, the feature at 820 cm^{-1} re-emerges as the Si–C stretch and becomes a well-defined peak upon annealing to 970 K (Fig. 6i), suggesting decomposition of the adspecies to SiC adspecies (and/or other hydrocarbon fragments) at these higher temperatures.

In addition, the C–H stretch feature at 2980 cm^{-1} (Fig. 6a) is found to gradually strengthen and evidently undergo a small red shift to 2900 cm^{-1}, while the CH bending feature at 1150 cm^{-1} weakens and becomes totally diminished, upon annealing to 450 K (Fig. 6d). These spectral changes are consistent with the thermal evolution of the proposed 1,2-dichlorovinyl adspecies to chlorovinylene (Structure VIII, Fig. 7d). The intensity of the red-shifted C–H stretch at

2900 cm^{-1} (Fig. 6d) remains essentially unchanged upon annealing to 700 K (Fig. 6f). At 850 K, however, this feature completely disappears, which is in accord with the breakdown of the chlorovinylene adspecies and the formation of the SiC adspecies (Fig. 7d) as reflected by the onset of the Si–C stretch feature at 820 cm^{-1} (Fig. 6g). Furthermore, the (*trans*-)1,2-dichlorovinyl adspecies (Structure VI, Fig. 7d) also appears to undergo direct double-dechlorination to acetylide (–C≡C–H, Structure IX, Fig. 7d) upon annealing to 450 K, which gives rise to the emergence of the C≡C stretch feature at 2080 cm^{-1} and the corresponding C–H stretch at 3300 cm^{-1}. The latter assignments are in good accord with similar frequencies observed for the model compound $Si(C{\equiv}CH)_4$, in which the C≡C stretch and C–H stretch are found to be at 2053/2063 cm^{-1} and 3315 cm^{-1}, respectively [37]. To the best of our knowledge, this represents the first observation of this novel acetylide adspecies on a semiconductor surface, although the presence of a surface-parallel acetylide as an intermediate structure has been proposed earlier in the case of metal surfaces [38–40]. Further annealing the sample to above 450 K appears to gradually reduce these intensities, suggesting thermal evolution of the acetylide adspecies to Si monohydrides and unknown hydrocarbon fragments (Fig. 7d). The Si–H stretch feature at 2080 cm^{-1} completely disappears upon annealing to above 700 K (Fig. 6f), confirming its assignment as monohydride. At the highest annealing temperature accessible in the present experiment (970 K), only the SiC adspecies remains, as indicated by the presence of the Si–C stretch at 820 cm^{-1} (Fig. 6i), and the Si sample exhibits a diffuse (partly reconstructed) 7×7 LEED pattern.

4. Summary

Unlike Si(1 0 0)2×1, the Si(1 1 1)7×7 surface provides a more challenging surface for exploration of silicon surface chemistry due to the large number of different bonding sites (adatoms, rest-atoms, dimer rows, corner holes, and pedestal atoms) on the surface [41]. In the present work, we employ EELS and TDS to investigate the RT chemisorption and plausible thermally driven chemical processes of PCE and its hydrogen-substituted homolog TCE on the Si(1 1 1)7×7 surface. In particular, molecular desorption near RT (350 K) has been observed as a minor pathway for the thermal evolution of PCE and TCE on the 7×7 surface, which provides support for the presence of dative covalent bonding (between Cl and the substrate Si atoms) as a result of the inductive effect of the Cl atoms (Structures I and V, Fig. 7). However, unlike the non-polar PCE adsorbate, the polar nature of the TCE molecule appears to provide sufficient adsorbate–substrate interaction to facilitate further double Cl abstraction by the substrate atoms (Fig. 7c), which leads to the thermal evolution of chloroacetylene (Fig. 4b). These molecular adsorption processes are plausible because the typical Cl-to-Cl separations along the C=C bond (3.1 Å) and diagonally across the molecule (4.4 Å) for PCE and TCE are physically compatible with the adatom-to-rest-atom separation (4.6 Å) and adatom–adatom separation across the dimer row (6.7 Å) on the 7×7 surface [28]. Furthermore, dechlorination of PCE and TCE is found to be the major pathway at RT on Si(1 1 1)7×7 (Fig. 7b and d). Although the complex mechanisms of these processes are beyond the scope of the present study, our data reveal the formation of novel products and intermediates upon annealing the samples. In particular, the observation of C=C stretch (near 1500 cm^{-1}) upon RT adsorption/dechlorination supports the presence of mono-σ bonded trichlorovinyl ($ClC{=}CCl_2$) adspecies for PCE (Structure III, Fig. 7b) and 1,2-dichlorovinyl ($ClC{=}CHCl$) adspecies for TCE (Structures VI and VII, Fig. 7d) as possible surface intermediates for further thermal evolution. Differences are also observed between PCE and TCE for the eventual evolution products upon annealing the samples above 450 K. For PCE, the absence of C–Cl stretch at ~820 cm^{-1} (Fig. 5c) suggests total dechlorination above 450 K, while the emergence of the Si–C stretch at 820 cm^{-1} (Fig. 5g) confirms the formation of SiC and C clusters adspecies (Fig. 7b). On the other hand, the small red-shift in the C–H stretch at 2980 cm^{-1} to 2900 cm^{-1} and the emergence of a new C–H stretch at 3300 cm^{-1} in the

TCE spectra (Fig. 6) indicate the presence of di-σ bonded chlorovinylene (HĊ=ĊCl, Structure VIII, Fig. 7d) and mono-σ bonded acetylide (–C≡C–H, Structure IX, Fig. 7d) adspecies. In addition to these novel adspecies, there are other viable pathways involving, e.g., the formation of chlorovinylidene (>C=CHCl, Structure X, Fig. 7d) that cannot be ruled out. All of these dechlorinated adspecies are found to undergo dehydrogenation upon further annealing the TCE sample to above 580 K, consistent with the increase followed by reduction in the Si–H stretch at 2080 cm^{-1} (Fig. 6) and the presence of mass 2 TDS feature commonly observed at 770–810 K from Si monohydrides [42,43]. The resulting adspecies undergo eventual formation of the SiC and C-containing clusters above 920 K, as for the PCE case (Fig. 6h). It should be noted that we cannot rule out more complicated surface processes involving multi-centers interactions and intermediate adspecies that are parallel to the surface, because these adspecies would escape detection by the specular-reflection EELS technique used in the present experiment. Despites these notable differences in the adsorption species, the Cl atoms dissociated from both PCE and TCE are found to desorb predominantly as an etching product $SiCl_2$ over 800–950 K and recombinatively with H as HCl over 700–900 K. Finally, the differences observed for the thermal evolution of PCE and TCE on Si(1 1 1)7×7 are clearly related to the adsorption geometries and symmetries of the adsorbates, which ultimately control the intricate site-specific surface chemistry of these novel adspecies on the 7×7 surface.

Acknowledgment

This work was supported by the Natural Sciences and Engineering Research Council of Canada.

References

[1] M.B. Moran, L.F. Johnson, Mater. Res. Soc. Sympos. Proc. 609 (2000) A23.2.
[2] Q.A. Huang, J.N. Chen, H.Z. Zhang, Q.Y. Tong, Jpn. J. Appl. Phys., Part 1 32 (1993) 2854.
[3] A.K Hochberg, A. Lagendijk, D.A. Roberts, R. Agny, B. Anders, R. Cotner, J. Jewett, J. Mulready, M. Tran, J. Electrochem. Soc. 139 (1992) L117.
[4] I.W. Boyd, R.B. Jackman, Photochemical Processing of Electronic Materials, second ed., Academic, London, 1992.
[5] W. Sesselman, T.J. Chuang, J. Vac. Sci. Technol. B3 (1985) 1507.
[6] X.H. Chen, J.C. Polanyi, D. Rogers, Surf. Sci. 376 (1997) 77.
[7] Y. Cao, J.F. Deng, G.Q. Xu, J. Chem. Phys. 112 (2000) 4759.
[8] P.H. Lu, J.C. Polanyi, D. Rogers, J. Chem. Phys. 111 (1999) 9905.
[9] P.H. Lu, J.C. Polanyi, D. Rogers, J. Chem. Phys. 112 (2000) 11005.
[10] Z.H. He, X. Yang, X.J. Zhou, K.T. Leung, Surf. Sci. 547 (2003) L840.
[11] X.J. Zhou, Q. Li, Z.H. He, X. Yang, K.T. Leung, Surf. Sci. 543 (2003) L668.
[12] R.A. Doong, K.T. Chen, H.C. Tsai, Environ. Sci. Technol. 37 (2003) 2575.
[13] D.Q. Hu, Ph.D. thesis, University of Waterloo, Waterloo, 1993.
[14] J.E. Demuth, B.N.J. Persson, A.J. Schell-Sorokin, Phys. Rev. Lett. 51 (1983) 2214.
[15] U. Backes, H. Ibach, Solid State Commun. 40 (1981) 575.
[16] B.N.J. Persson, J.E. Demuth, Phys. Rev. B 30 (1984) 5968.
[17] T. Shimanouchi, Tables of molecular vibrational frequencies consolidated volume I, National Bureau of Standards, Gaithersburg, 1972, p. 1.
[18] K.S. Pitzer, J.L. Hollenberg, J. Am. Chem. Soc. 76 (1954) 1439.
[19] G. Allen, H.J. Berstein, Can. J. Chem. 32 (1954) 1044.
[20] T.J. Houser, R.B. Berstein, R.G. Miekka, J.C. Angus, J. Am. Chem. Soc. 77 (1955) 6201.
[21] J. Schmidt, C. Stuhlmann, H. Ibach, Surf. Sci. 302 (1994) 10.
[22] Q. Gao, C.C. Cheng, P.J. Chen, W.J. Choyke, J.T. Yates Jr., J. Chem. Phys. 98 (1993) 8308.
[23] J.M. Buriak, Chem. Rev. 102 (2002) 1271.
[24] R.T. Sanderson, Polar Covalence, Academic, New York, 1983.
[25] R.T. Sanderson, Chemical Bonds and Bond Energy, second ed., Academic, New York, 1976.
[26] M.X. Yang, S. Sarkar, B.E. Bent, S.R. Bare, M.T. Holbrook, Langmuir 13 (1997) 229.
[27] J. Yoshinobu, D. Fukushi, M. Uda, E. Nomura, M. Aono, Phys. Rev. B 46 (1992) 9520.
[28] S.Y. Tong, H. Huang, C.M. Wei, W.E. Pachard, F.K. Men, G. Glander, M.B. Webb, J. Vac. Sci. Technol. A 6 (1988) 615.
[29] D.R. Lide (Ed.), CRC Handbook of Chemistry and Physics, 85th ed., CRC Press, Boca Raton, 2005.
[30] H. Ibach, H.D. Bruchmann, H. Wagner, Appl. Phys. A 29 (1982) 113.
[31] J.J. Boland, J.S. Villarrubia, Science 248 (1990) 838.

[32] Eight Peak Index of Mass Spectra, vol. 1, Mass Spectrometry Data Center, Aldermaston, 1974.
[33] P.A. Coon, P. Gupta, M.L. Wise, S.M. George, J. Vac. Sci. Technol. A 10 (1992) 324.
[34] D.D. Koleske, S.M. Gates, D.B. Beach, J. Appl. Phys. 72 (1992) 4073.
[35] K.H. Junker, G. Hess, J.G. Eherdt, J.M. White, J. Vac. Sci. Technol. A 16 (1998) 2995.
[36] H. Ibach, H. Wagner, D. Bruchmann, Solid State Commun. 42 (1982) 457.
[37] S.C. Laroze, S. Haq, R. Raval, Y. Jugnet, J.C. Bertolini, Surf. Sci. 433–435 (1999) 193.
[38] J. Yoshinobu, H. Tsuda, M. Onchi, M. Nishijima, Solid State Commun. 60 (1986) 801.
[39] Y. Jugnet, J.C. Bertolini, L.A.M.M. Barbosa, P. Sautet, Surf. Sci. 505 (2002) 153.
[40] L.A.M.M. Barbosa, P. Sautet, J. Catal. 207 (2002) 127.
[41] H.N. Waltenburg, J.T. Yates Jr., Chem. Rev. 95 (1995) 1589.
[42] K. Oura, V.G. Lifshits, A.A. Saranin, A.V. Zotov, M. Katayama, Suf. Sci. Rep. 35 (1999) 1.
[43] R.M. Wallace, P.A. Taylor, W.J. Choyke, J.T. Yates, Surf. Sci. 239 (1990) 1.